RESEARCH ARTICLE

The flavonoid tangeretin activates the unfolded protein response and synergizes with imatinib in the erythroleukemia cell line K562

Sofie Lust[1,2], Barbara Vanhoecke[2], Mireille Van Gele[3], Jan Philippé[4], Marc Bracke[2] and Fritz Offner[1]

[1] Department of Hematology, University Hospital Ghent, Ghent, Belgium
[2] Laboratory of Experimental Cancer Research, Department of Radiation Oncology and Experimental Cancer Research, University Hospital Ghent, Ghent, Belgium
[3] Department of Dermatology, University Hospital Ghent, Ghent, Belgium
[4] Departments of Clinical Chemistry, Microbiology and Immunology, University Hospital Ghent, Ghent, Belgium

Received: April 27, 2009
Revised: June 16, 2009
Accepted: July 5, 2009

We explored the mechanism of cell death of the polymethoxyflavone tangeretin (TAN) in K562 breakpoint cluster region-abelson murine leukemia (Bcr-Abl+) cells. Flow cytometric analysis showed that TAN arrested the cells in the G_2/M phase and stimulated an accumulation of the cells in the sub-G_0 phase. TAN-induced cell death was evidenced by poly(ADP)-ribose polymerase cleavage, DNA laddering fragmentation, activation of the caspase cascade and down-regulation of the antiapoptotic proteins Mcl-1 and Bcl-x_L. Pretreatment with the pancaspase inhibitor Z-VAD-FMK_blocked caspase activation and cell cycle arrest but did not inhibit apoptosis which suggest that other cell killing mechanisms like endoplasmic reticulum (ER)-associated cell death pathways could be involved. We demonstrated that TAN-induced apoptosis was preceded by a rapid activation of the proapoptotic arm of the unfolded protein response, namely PKR-like ER kinase. This was accompanied by enhanced levels of glucose-regulated protein of 78 kDa and of spliced X-box binding protein 1. Furthermore, TAN sensitized K562 cells to the cell killing effects of imatinib *via* an apoptotic mechanism. In conclusion, our results suggest that TAN is able to induce apoptosis in Bcr-Abl+ cells *via* cell cycle arrest and the induction of the unfolded protein response, and has synergistic cytotoxicity with imatinib.

Keywords:
Apoptosis / Cell cycle arrest / Flavonoid / Imatinib / Unfolded protein response

1 Introduction

Flavonoids are widely distributed polyphenolic compounds in plants and in food. They exhibit a wide variety of biological effects including antioxidative, antiangiogenic, anti-invasive, antiproliferative and anti-inflammatory activities [1]. Tangeretin (TAN) is a polymethoxyflavone naturally present in citrus peel oil. TAN has been studied in breast cancer cells by Bracke *et al.* [2–4], who demonstrated that TAN inhibits invasion and proliferation of MCF-7/6 cells at least in part by affecting cell–cell interactions. TAN also exerts antiproliferative effects in lung carcinoma cells [5], in colorectal carcinoma cells [6] and in lymphoid cell lines (HL-60) [7] at 10^{-4} M *in vitro*. Recently, an increasing number of reports link flavonoid-induced cell death to the induction of endoplasmic reticulum (ER) stress [8, 9].

Correspondence: Professor Fritz Offner, Department of Hematology, University Hospital Ghent, De Pintelaan 185, 9K12IE, 9000 Ghent, Belgium
E-mail: Fritz.Offner@ugent.be
Fax: +32-9-332-2737

Abbreviations: AnnV, annexin V; **ATF,** activating transcription factor; **BA,** brefeldin A; **Bcr-Abl,** breakpoint cluster region-abelson murine leukemia; **CHOP,** C/EBP homologous protein-10; **CI,** combination index; **CML,** chronic myelogenous leukemia; **DAPI,** 4′-6-diamidino-2-phenylindole; **eIF2α,** eukaryotic translation initiation factor 2; **ER,** endoplasmic reticulum; **GRP78,** glucose-regulated protein of 78 kDa; **IRE1,** inositol-requiring enzyme 1; **LC,** living cells; **MTT,** 3-(4,5-dimethylthiazol-2-yl)-2,5-diphenyl-tetrazoliumbromide; **PARP,** poly(ADP)-ribose polymerase; **PERK,** PKR-like ER kinase; **PI,** propidium iodide; **TAN,** tangeretin; **TG,** thapsigargin; **UPR,** unfolded protein response; **XBP1,** X-box binding protein 1

The accurate function of the ER plays a crucial role in securing cell survival. Therefore, the cell has developed rescue mechanisms, namely the unfolded protein response (UPR) and the ER-associated protein degradation in order to cope with ER stress. Under ER stress, unfolded or misfolded proteins accumulate in the ER lumen and/or the ER calcium homeostasis is disrupted, which triggers the UPR. This stress response is characterized by a strong upregulation of the ER-resident chaperone GRP78/BiP (glucose-regulated protein of 78 kDa). GRP78 controls the three ER stress-transducers, namely the activating transcription factor 6 (ATF6), the inositol-requiring enzyme 1 (IRE1) and PKR-like ER kinase (PERK). When the UPR fails to reverse prolonged ER stress this will ultimately lead to programmed cell death *via* mitochondria-dependent or -independent pathways [10].

Chronic myelogenous leukemia (CML) is characterized by the presence of the Philadelphia chromosome which is the product of a reciprocal translocation between chromosome 9 and 22. As a consequence, a fusion protein, namely breakpoint cluster region-abelson murine leukemia (Bcr-Abl), is formed which leads to the constitutive activation of the Abl tyrosine kinase [11]. Selective tyrosine kinase inhibitors of Bcr-Abl, such as imatinib, dasatinib and nilotinib, are among the most successful non-chemotherapeutic agents used in current CML treatments. However, resistance to current therapies is emerging, making new drug development and/or combination treatments necessary.

In this study, we show for the first time that TAN induces activation of the proapoptotic arm of the UPR and cell cycle arrest in Bcr-Abl+ cells. Moreover, we demonstrate that TAN enhances the cell killing effect induced by imatinib.

2 Materials and methods

2.1 Cell culture

The human erythroleukemia cell line K562 was obtained from American Type Culture Collection (ATCC). K562 cells were cultured in suspension in RPMI1640 medium supplemented with 10% fetal bovine serum (Greiner bio-one, Wemmel, Belgium), 100 IU/mL penicillin, 100 μg/mL streptomycin and 0.56 μg/mL fungizone (Gibco BRL, Merelbeke, Belgium) and kept at 37°C in a humidified atmosphere of 5% CO_2 in air.

2.2 Chemicals and antibodies

Purified 5,6,7,8,4′-pentamethoxyflavone (TAN) was kindly provided by the Department of Citrus Lakeland (Florida, USA). TAN was dissolved in DMSO as a stock solution of 10^{-2} M, from which further dilutions were made. Z-VAD-FMK (stock: 100 mM), and the ER stress inducers brefeldin A (BA) (stock: 2.5 mg/mL) and thapsigargin (TG) (stock: 1 mM) were dissolved in DMSO, and were respectively from BD Biosciences (Erembodegem, Belgium) and Sigma (Bornem, Belgium). For western blot following primary antibodies were used: rabbit anti-cleaved caspase-3 (Asp175) from Cell Signaling Technology (Beverly, MA, USA), rabbit anti-Bax, anti-Mcl-1, anti-GRP78, anti-X-box binding protein 1 (anti-XBP1), mouse anti-Bcl-x_L, anti-CHOP (C/EBP homologous protein-10) from Santa Cruz Biotechnology (Santa Cruz, CA, USA), mouse anti-eukaryotic translation initiation factor 2 (anti-eIF2α) and rabbit anti-phospho-eIF2α (Ser52) from Biosource (Nevele, Belgium), rabbit anti-caspase-8, mouse anti-Bak, anti-caspase-7, anti-poly(ADP)-ribose polymerase (anti-PARP) from BD Biosciences (San Diego, USA), mouse anti-caspase-9 from Stressgen (Victoria, Canada), anti-α-tubulin from Sigma, goat anti-Bid from R&D systems (Immuno-Source, Halle, Belgium) and mouse anti-procaspase-3 from Abcam (Cambridge, UK).

2.3 MTT assay

The mitochondrial activity of K562 cells was measured using the 3-(4,5-dimethylthiazol-2-yl)-2,5-diphenyl-tetrazoliumbromide (MTT) assay. Cells were seeded in triplicate in 96-well plates and treated with various concentrations of TAN. Incubation was performed at 37°C for 24 h until 96 h. After treatment, MTT solution (5 mg/mL) was added in each well and incubated overnight at 37°C. Formazan was dissolved in DMSO and measured at 490 nm in a multiplate reader. The IC_{50} was extrapolated from polynomial regression analysis of experimental data.

2.4 Cytospin and May–Grünwald–Giemsa staining

Cells were spun onto a microscope slide for 5 min at 400 g under medium acceleration in a cytospin centrifuge. After air drying, slides were stained with May–Grünwald–Giemsa (Sigma) by a Mirastainer (Merck, Darmstadt, Germany) according to the manufacturer and observed under the microscope. Mitotic cells were analyzed and expressed as mitotic cell counts. At least 100 cells were counted for each condition. Each condition was tested in duplicate in two independent experiments.

2.5 Fluorescence microscopy

After treatment, cells were washed once with PBS followed by fixation in cold methanol for 15 min. After fixation, cells were washed with PBS prior to staining with 4′-6-diamidino-2-phenylindole (DAPI; Sigma) in the dark at room temperature for 15 min. Before analyzing the cells by Carl Zeiss Axio Vision microscope, cells were washed with PBS.

2.6 DNA fragmentation assay

DNA from K562 cells treated with 1% DMSO, 50 or 100 μM TAN for 12, 24 and 48 h was extracted using the Suicide Track DNA Ladder Isolation kit (Calbiochem, San Diego, CA). Samples were analyzed on a 1.5% agarose gel. A positive DNA ladder control (HL-60 cells treated with 0.5 mg/mL actinomycin D for 19 h) was supplied with the kit.

2.7 Western blot analysis

After treatment for different times, cell lysates were prepared and immunostaining of the blots was performed as described previously [12]. Proteins were separated by gel electrophoresis on a 10 or 16% polyacrylamide gel and transferred onto nitrocellulose membranes. Immunostaining of the blots was done using primary antibodies, followed by the horseradish peroxidase-conjugated secondary antibody and detection was performed using the chemiluminescence ECL kit (GE Healthcare, Diegem, Belgium). Quantification of the autoradiograms was done using the Quantity One Software (Bio-Rad, Eke, Belgium).

2.8 Flow cytometric analysis

K562 cells were cultured in duplicate for 24 and 48 h. After treatment, cells were washed once with ice-cold PBS and collected by centrifugation. After staining with annexin V (AnnV)–FITC and propidium iodide (PI) (human AnnV–FITC detection kit, Bender MedSystems Diagnostics, Vienna, Austria), the percentage of living cells (LC) was assessed by flow cytometry. For analysis of the cell cycle distribution, the Coulter® DNA Prep™ Reagents Kit (Beckman Coulter, Fullerton, CA, USA) was used according to the manufacturer's recommendations. After treatment, cells were washed with PBS and exposed to DNA Prep LPR for 1 min, followed by incubation with DNA Prep Stain for 15 min at room temperature. Flow cytometric analysis was performed on a Beckman Coulter Cytomics FC500 flow cytometer (Beckman Coulter). Cell cycle fractions (G_0/G_1, S and G_2/M) were quantified using WinCycle software (Phoenix Flow Systems, San Diego, CA, USA) while the sub-G_0 fractions was quantified manually.

2.9 RT-PCR and real-time quantitative RT-PCR

Total RNA was extracted from K562 cells using the RNeasy Mini Kit (Qiagen, Venlo, The Netherlands) according to the manufacturer's instructions. DNase treatment, cDNA synthesis and SYBR Green I reverse transcription-PCR were performed as described previously [13, 14] (http://genomebiology.com/2002/3/7/research/0034.1). The primer sequences are available from the real-time PCR primer and Probe Database (gene: primer-ID; *HSPA5* (*GRP78*): 3477) [15]. The comparative Ct method was used for quantification. To correct for differences in RNA quantities and cDNA synthesis efficiency, relative gene expression levels were normalized using the geometric mean of three housekeeping genes (*RPL13A*, *UBC* and *HPRT1*) according to Vandesompele *et al.* [14]. The normalized expression level (%) of *GRP78* of each treated sample was compared with that of its corresponding untreated one (solvent control) at a particular time point.

To amplify the fragments coding for *XBP1*(*u*) and *XBP 1*(*s*), we selected a primer set described by Ding *et al.* [16]. PCR reactions were performed in a 1x TaKaRa ExTaq™ PCR reaction mixture (TaKaRa Bio, Shiga, Japan) according to the manufacturer's instructions. PCR amplifications were performed for 35 cycles on a PTC-0150 Minicycler (Bio-Rad) using the following cycling parameters: 95°C for 30 s, 60°C for 30 s and 72°C for 1 min with a final extension period of 72°C for 10 min. Samples were loaded on a 3% agarose gel.

RNA isolation and cDNA preparation of the *BCR-ABL* fusion gene was performed as follows. Total cellular RNA was extracted with the Trizol method (Invitrogen, Merelbeke, Belgium) and cDNA was synthesized from 1 μg RNA with the Eurogentic Reverse Transcription Core Kit (Eurogentec, Seraing, Belgium) according to the manufacturer's instructions. PCR amplification was performed by an iCycler™ Real-Time Detection System (Bio-Rad) using the qPCR™ Core Kit (Eurogentec) and following cycling parameters (50 cycli): 95°C for 15 s, 60°C for 30 s and 60°C for 30 s with a final extension period of 25°C for 2 min. Primer sequences are summarized in Table 1.

Table 1. Primer sequences used in the RT-PCR and real-time Q-PCR

Name of the primer	Primer sequences
XBP-1 FW	TGGTTGCTGAAGAGGAGGCGGAAG
XBP-1 REV	GAAAAGGGAGGCTGGTAAGGAAC
GRP78 FW	GGCCGCACGTGGAATG
GRP78 REV	ACCTCCAATATCAACTTGAATGTATGG
ENF501 BCR	TCCGCTGACCATCAAYAAGGA
ENR561 ABL	CACTCAGACCCTGAGGCTCAA
ENF402 BCR	CTGGCCCAACGATGGCGA
ENF1003 CG-ABL (house)	TGGAGATAACACTCTAAGCATAACTAA AGGT
ENR1063 CG-ABL (house)	GATGTAGTTGCTTGGGACCCA
ENP541 BCR-ABL	CCCTTCAGCGGCCAGTAGCATCTGA
ENP2 1043 CG-ABL (house)	CCATTTTTGGTTTGGGCTTCACACCATT

CG-ABL (house), control gene abelson gene; ENF, European network forward primer; ENP, European network Taqman probe; ENR, European network reverse primer; FW, forward; REV, reverse.

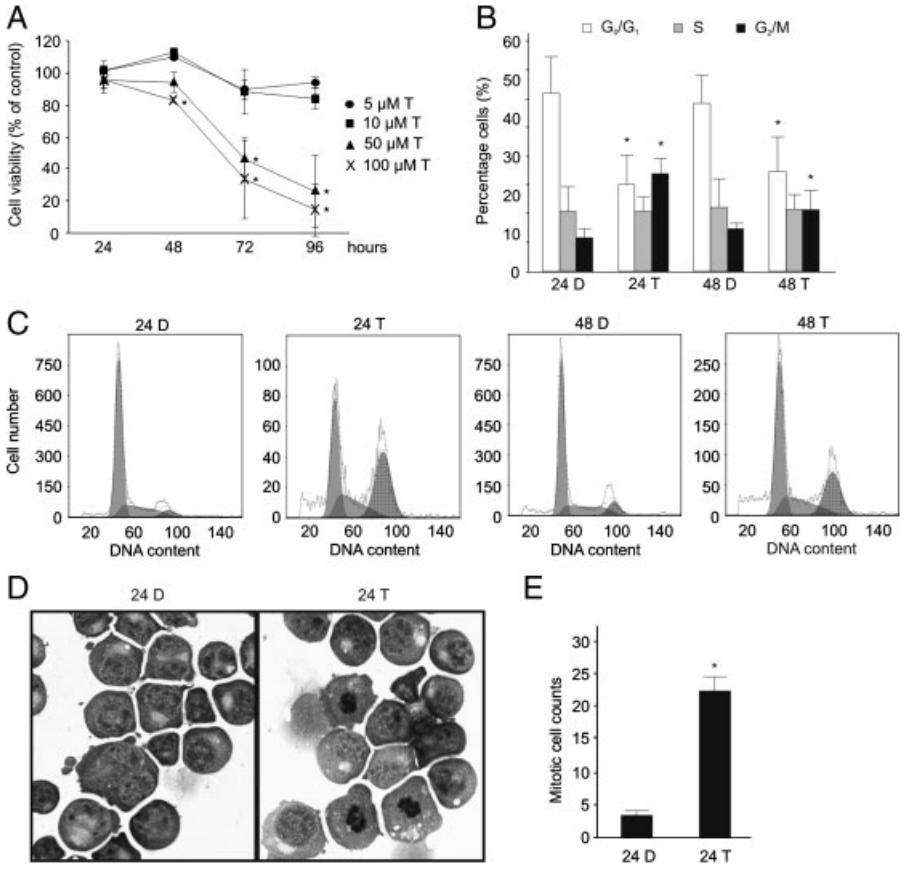

Figure 1. TAN inhibits cell proliferation in K562 cells. (A) Several concentrations of TAN were tested for 24–96 h using the MTT assay. Data are expressed as percentage cell viability of control and each value is the result of three independent experiments. The graph (B) and histograms (C) of the cell cycle progression are presented. K562 cells were incubated with 100 μM TAN for 24 and 48 h. The mean percentage cells in each phase of the cell cycle of five independent experiments are shown. (D) May–Grünwald–Giemsa-stained cytospin slides were prepared of K562 cells that were treated with 100 μM TAN for 24 h. The cytospins were viewed under the microscope using a × 50 oil objective and representative fields are shown. (E) Quantification of the mitotic cell counts on 100 cells *per* condition. The result is the mean of two independent experiments. Error bars indicate the SD and the asterisk denotes a significant difference of $p < 0.05$ (*).

2.10 Data analysis

Data are presented as the mean ± SD for two separate experiments. Statistical analysis of the data between treated and solvent control group was performed with Student's *t*-test and a *p*-value less than 0.05 was considered significant. The synergistic effect of imatinib and TAN on K562 cells was analyzed using the median dose analysis of a commercially available software program (CalcuSyn, Biosoft, Ferguson, MO, USA) [17, 18]. A combination index (CI) less than 1 indicated synergism and a CI greater than 1 indicated antagonism.

3 Results

3.1 TAN impairs proliferation *via* G_2/M arrest without affecting differentiation of K562 cells

In order to investigate the antiproliferative potential of TAN in K562 cells, the MTT assay was performed. Figure 1A shows that TAN reduced the mitochondrial activity of K562 cells in a dose- and time-dependent way. The IC_{50} value was 42.4 ± 13.6 and 31.2 ± 6.4 μM after 72 and 96 h treatment, respectively. In order to reveal the mechanism behind this antiproliferative effect, the influence of TAN on the cell cycle progression of K562 cells was assessed. The cells were treated with 1% DMSO (solvent control) or with 100 μM TAN for 24 and 48 h and analyzed *via* flow cytometry and cytospins. The percentage of cells in G_0/G_1, S and G_2/M phase, and the histograms of flow cytometric analysis are shown in Figs. 1B and C, respectively. After 24 h, TAN-induced a G_2/M arrest in 34.1 ± 5.2% of the treated cells compared with 11.7 ± 3.2% of the solvent-treated cells. In addition, the G_0/G_1 phase fraction decreased from 62.0 ± 12.8% in the control condition to 30.2 ± 10.1% cells in the treated group while the S-phase was unchanged. Moreover, the sub-G_0 phase fraction increased in the treated group (14.3 ± 4.5) compared with cells in the control group (5.8 ± 2.8). A similar increase in the sub-G_0 and G_2/M phase could be noticed after longer treatment. The appearance of a sub-G_0 fraction after 24 and 48 h treatment with TAN is suggestive of an apoptotic cell death mechanism. The influence of 100 μM TAN on the morphology of K562 cells was evaluated by a cytospin preparation stained by May–Grünwald–Giemsa. Mitotic arrest in the metaphase stage could be noticed in the TAN-treated cultures compared with control cultures (Fig. 1D). Quantitative analysis of the mitotic cell counts is shown in Fig. 1E. Finally, the influence of TAN on the differentiation status of the K562 cells was analyzed. It is known that K562 cells differentiate into erythroid precursors as was shown for treatment with imatinib [19] and cyclosporine A [20], or to megakaryocytic

lineages after treatment with phorbol 12-myristate 13-acetate [21]. Therefore, K562 cells were incubated for 4 days with 10 μM TAN and stained for glycophorin A (a marker for erythroid cells), CD33 and CD31 (a marker for monocytic cells) and CD61 (a marker for megakaryocytes). However, no stimulation of differentiation could be observed (data not shown).

3.2 TAN induces apoptosis in K562 cells

The increase in sub-G_0 fraction is suggestive of an apoptosis-like cell death mechanism. Therefore, we performed AnnV–PI staining followed by flow cytometry after treatment of K562 cells with 50 or 100 μM TAN for 24 and 48 h. Figure 2A shows that the mean percentage of LC decreased in a dose- and time-dependent way. Although a minor downregulation was noticed with 50 μM TAN after 24 h, a significant decrease could be noticed after 48 h (55.4 ± 8.7% LC) compared with solvent control (95.0 ± 6.8% LC). However, 100 μM TAN induced cell death already after 24 h (75.3 ± 9.1% LC for treated culture; 97.5 ± 12.3% LC for control culture) and was more pronounced after 48 h (44.4 ± 11.3% LC for treated culture; 93.8 ± 5.4% LC for control culture). Furthermore, we examined other characteristics of an apoptotic cell death mechanism namely

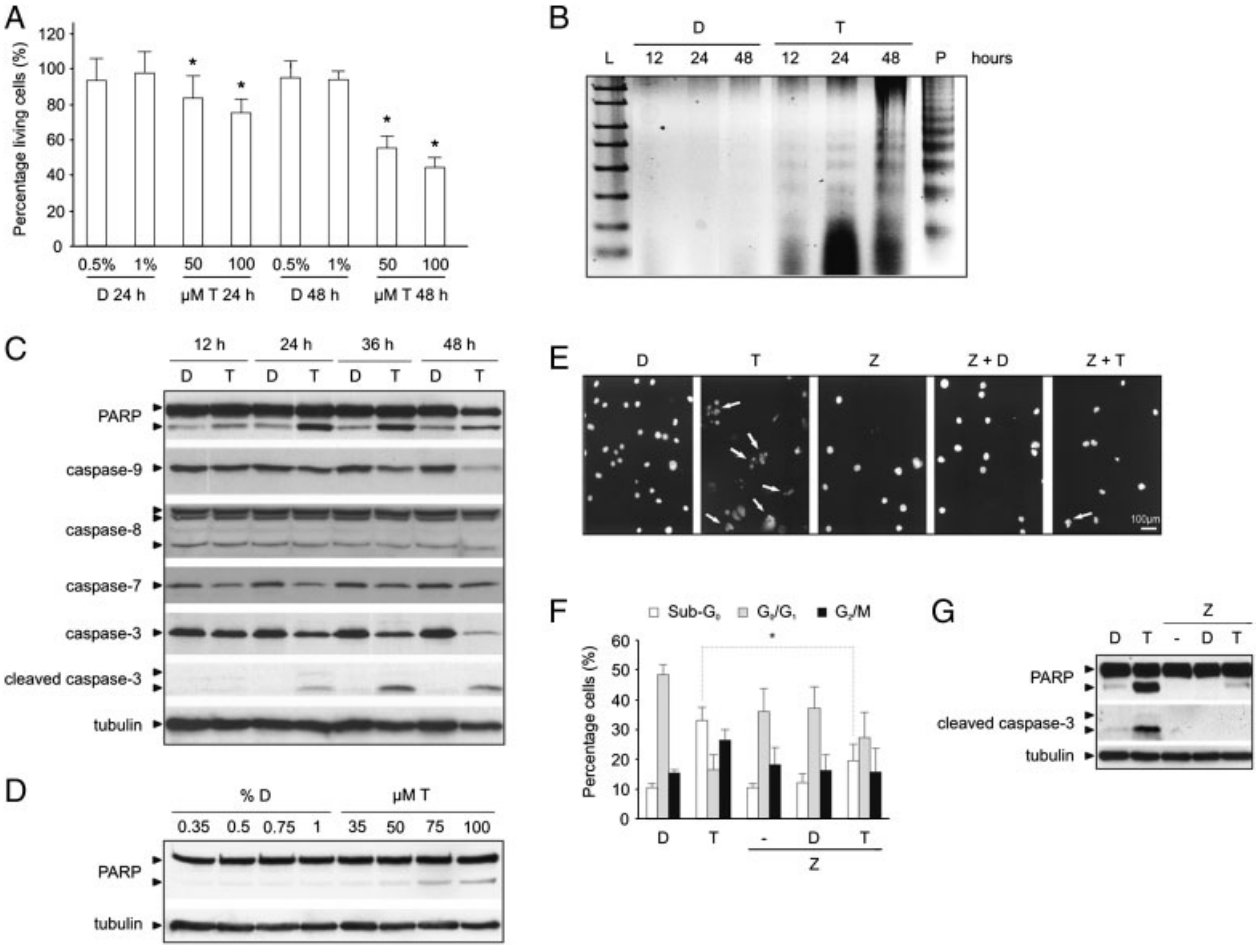

Figure 2. TAN induces cell death *via* an apoptotic mechanism. (A) The mean percentage LC of six independent experiments was determined after 24 and 48 h treatment with 50 and 100 μM TAN or corresponding solvent control concentration (DMSO). (B) Exposure of K562 cells to 100 μM TAN or 1% DMSO for 12, 24 and 48 h resulted in the appearance of a DNA laddering pattern. (C) Lysates were prepared after different time periods. K562 cells were treated with 100 μM TAN or solvent control (DMSO) and membranes were stained for procaspase-9, -8, -7, -3, cleaved caspase-3 and tubulin as loading control. A dilution of TAN resulted in cleavage of PARP after 24 h treatment. One representative blot is shown in (C) and (D). The effect of TAN on the formation of apoptotic bodies was determined *via* fluorescence microscopy. K562 cells were treated for 24 h with 100 μM TAN, or solvent and/or pretreated for 1 h with 50 μM Z-VAD-FMK. After the incubation period, cells were stained with DAPI (E). Simultaneously, the mean percentage cells of three independent experiments in each stage of the cell cycle and the effect on PARP and cleaved caspase-3 were determined, respectively *via* flow cytometry (F) and *via* western blot (G). One representative blot is illustrated. Error bars present the SD and a significant difference of $p < 0.05$ (*) is shown.

DNA laddering fragmentation, PARP cleavage, processing of caspases and cell morphology. TAN-induced apoptosis was evidenced by DNA laddering fragmentation starting from 100 μM TAN after 24 and 48 h treatment (Fig. 2B). Furthermore, as shown in Fig. 2C, 100 μM TAN induced PARP cleavage already after 12 h. After 24 h, PARP cleavage was considerably enhanced, starting from 75 μM (Fig. 2D). In addition, 100 μM TAN resulted in a decrease of procaspase-7 and procaspase-3 after 12 h accompanied by a minor decrease in procaspase-9, which was more apparent after 24 h. In contrast, no activation of caspase-8 could be detected (Fig. 2C). One of the key morphological features of late stage apoptosis is the appearance of apoptotic bodies which could be visualized by a DAPI-staining of K562 cells treated for 24 h with 100 μM TAN (Fig. 2E).

To find out if the effect of TAN on cell death was caspase-dependent, the pancaspase inhibitor Z-VAD-FMK was used. Pretreatment with 50 μM Z-VAD-FMK significantly reduced the sub-G_0 population, *e.g.* 32.9 ± 4.6% cells in TAN-treated cells in contrast to 19.4 ± 5.7% cells in Z-VAD-FMK-pretreated cells, induced no G_2/M arrest and a minor decrease in G_0/G_1 phase compared with TAN-treated cells (Fig. 2F). Moreover, PARP cleavage and caspase-3 activation were abolished after 24 h of cotreatment (Fig. 2G) but cell death was not completely inhibited (data not shown). DAPI staining confirmed these results (Fig. 2E).

3.3 TAN modulates expression of the Bcl-2 family members in K562 cells

The Bcl-2 family members play an important role in the regulation of cell death by controlling the release of apoptogenic factors from the mitochondria [22]. The expression of the proapoptotic proteins (Bak, Bax and Bid) and the antiapoptotic proteins (Mcl-1 and Bcl-x_L) was monitored following treatment with TAN (Fig. 3). Exposure of K562 cells to 100 μM TAN for different treatment times resulted in downregulation of Mcl-1 and Bcl-x_L starting from 12 h while Bax levels were decreased and a minor decrease in Bid could be noticed after 24 h of treatment. Bak levels were unchanged after TAN treatment.

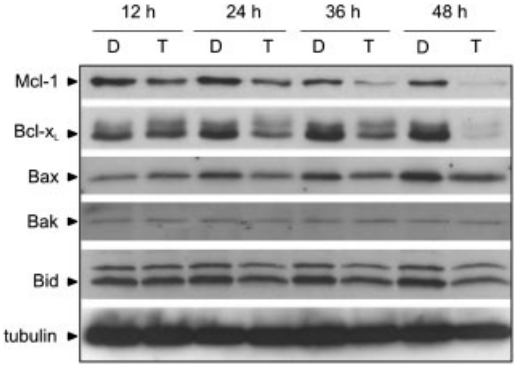

Figure 3. Modulation of the Bcl-2 family by TAN. Lysates of K562 cells treated with 100 μM TAN or solvent control (DMSO) were prepared after several time points and analyzed *via* western blot using antibodies for Bak, Bax, Bcl-x_L, Bid, Mcl-1 and tubulin (used as loading control). One representative blot is illustrated.

3.4 TAN activates the UPR in K562 cells

We hypothesized that other processes like ER stress-mediated cell death may be involved during TAN-induced apoptosis. To test the involvement of the UPR, we first examined the GRP78 expression levels by real-time quantitative RT-PCR and western blot. Upon treatment with TAN, *GRP78* mRNA levels rose considerably from 12 h on (Fig. 4A) and this was confirmed on protein level after 24 and 48 h (Fig. 4B). The activation of IRE1 and PERK was indirectly measured by examining their effect on their respectively downstream targets namely splicing of XBP1 and phosphorylation of eIF2α. To study the effect of TAN on XBP1 splicing, RT-PCR and western blot were performed as described in Section 2. Figure 4C shows that exposure to TAN induced splicing of *XBP1* mRNA after 12 and 24 h resulting in an increase of the corresponding protein (XBP1(s)) as shown in Fig. 4D. The well-known ER stress inducers BA and TG were used as positive control. Activation of PERK was analyzed by measurement of the phosphorylation levels of eIF2α. An increase could be noticed starting from 3 h of treatment which was sustained until 24 h. In contrast, total eIF2α remained unchanged. Phosphorylation of eIF2α results in a global protein translation block, although the translation of certain mRNAs, such as *ATF4*, is selectively upregulated. Upregulation of ATF4 results in the elevated expression of the proapoptotic protein C/EBP homologous protein-10 (CHOP). In our experiment, the transcription factor ATF4 was upregulated starting from 3 h, followed by a considerable increase of CHOP starting from 6 h of treatment with TAN (Fig. 4E). The higher band of ATF4 represents a different isoform of ATF4 and isoforms ranging from 30 to 50 kD have been reported during ER stress [23].

3.5 TAN synergizes with imatinib in inducing cell death in K562 cells

Since the oncogenic *BCR-ABL* fusion gene is responsible for the abnormal proliferation and survival signals leading to CML [11], we examined the effect of TAN on Bcr-Abl expression. Therefore, a real-time quantitative RT-PCR was performed with 100 μM TAN at different times (24 and 48 h). However, Fig. 5A illustrates that TAN did not have an effect on *BCR-ABL* mRNA levels. To assess the effect of cotreatment of TAN and imatinib, K562 cells were exposed to different concentrations of imatinib (0.4, 0.8, 1.6 and 3.2 μM) and of TAN (10, 20, 40 and 80 μM) at a constant ratio of 1/25 for 24, 48 and 72 h. The percentage of LC and

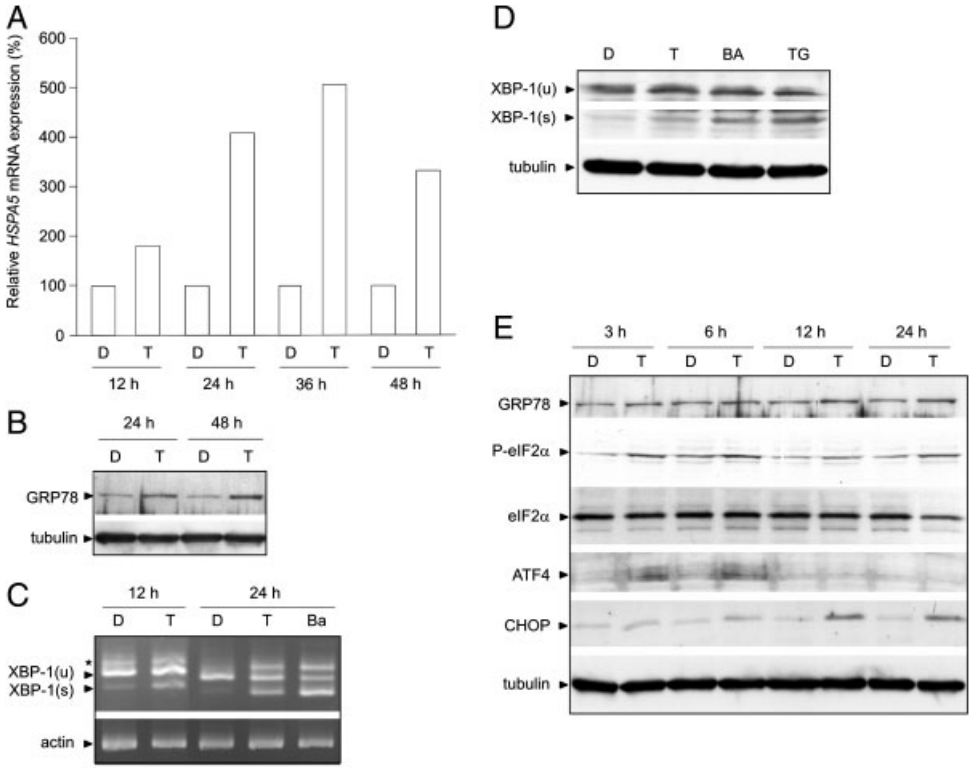

Figure 4. TAN activates the UPR to induce cell death in K562 cells. K562 cells were treated with 100 μM TAN or with 1% DMSO (solvent control) for different incubation periods. (A) Real-time quantitative RT-PCR was performed to analyze *GRP78* mRNA expression. The effect on *GRP78* mRNA level was confirmed *via* western blot (B). Splicing of the ER stress-induced XBP1 was analyzed *via* PCR reaction and western blot. (C) After the amplification reaction, samples were loaded on a 3% agarose gel to distinguish unspliced *XBP1* (312 bp) and spliced *XBP1* (286 bp). As positive control K562 cells were treated with 10 μg/mL BA during 24 h. The asterisk (*) represents an aspecific band of *XBP1*. (D) K562 cells were treated with TAN and the ER stress inducers BA (10 μg/mL) and TG (1 μM) during 6 h. The membrane was stained with XBP1. (E) Lysates were further analyzed *via* western blot for ATF4, CHOP, total and phospho-eIF2α, and GRP78. Tubulin was used as loading control. One representative gel and blot are shown.

dead cells (= fraction affected cells) was assessed on flow cytometry by AnnV–PI double staining. The fraction affected cells were used to determine the CI *via* the software program CalcySyn. CI values lower than 1 corresponded to a synergistic effect. As such, synergistic interactions between imatinib and TAN could be demonstrated after 48 h of treatment (Figs. 5B and C). In addition, the effect of the cotreatment and the single drugs on caspase activation was evaluated. Figure 5D shows that imatinib and TAN alone already induced cleavage of PARP and activation of caspase-3 and -9 after 24 h. However, cotreatment enhanced the effect and confirmed the synergistic effect of imatinib and TAN. Moreover, the effect of both drugs on cell morphology and the cell cycle were analyzed by May–Grünwald–Giemsa-stained cytospins. Figure 5E shows that after 24 h imatinib induced clearly detectable morphological changes of erythroid differentiation of K562 cells compared with untreated cells, while figures of a mitotic arrest could be detected in the TAN-treated cells. Cotreatment of TAN and imatinib induced a mitotic arrest and appearance of apoptotic bodies in K562 cells. Quantitative analysis of mitotic cell counts confirmed these results (Fig. 5F).

4 Discussion

Bcr-Abl+ leukemia is characterized by the activation of different signal transduction pathways that confer a survival advantage, promote proliferation and migration. New drug development in this disease primarily focuses on specific inhibitors of the *BCR-ABL* fusion gene. Since mutants will continue to develop, the development of alternatives remains an important topic. Therefore, interactions between the Bcr-Abl tyrosine kinase inhibitor, *e.g.* imatinib and other potential target candidates are attractive strategies to overcome imatinib-resistance.

The aim of this study was to investigate the molecular mechanism of TAN in the Bcr-Abl+ K562 cell line. Previous reports already demonstrated the antiproliferative potential of TAN in cancer cells *in vitro* in colorectal carcinoma cells [6] and in the promyelocytic leukemia HL-60 cell line [7]. In this study, we show that TAN suppressed the proliferation of K562 cells through a G_2/M arrest. In addition, it stimulated the accumulation of cells in the sub-G_0 fraction, suggestive for an apoptotic cell death mechanism. TAN-induced apoptosis was confirmed by the processing of caspase-3, -7, -9,

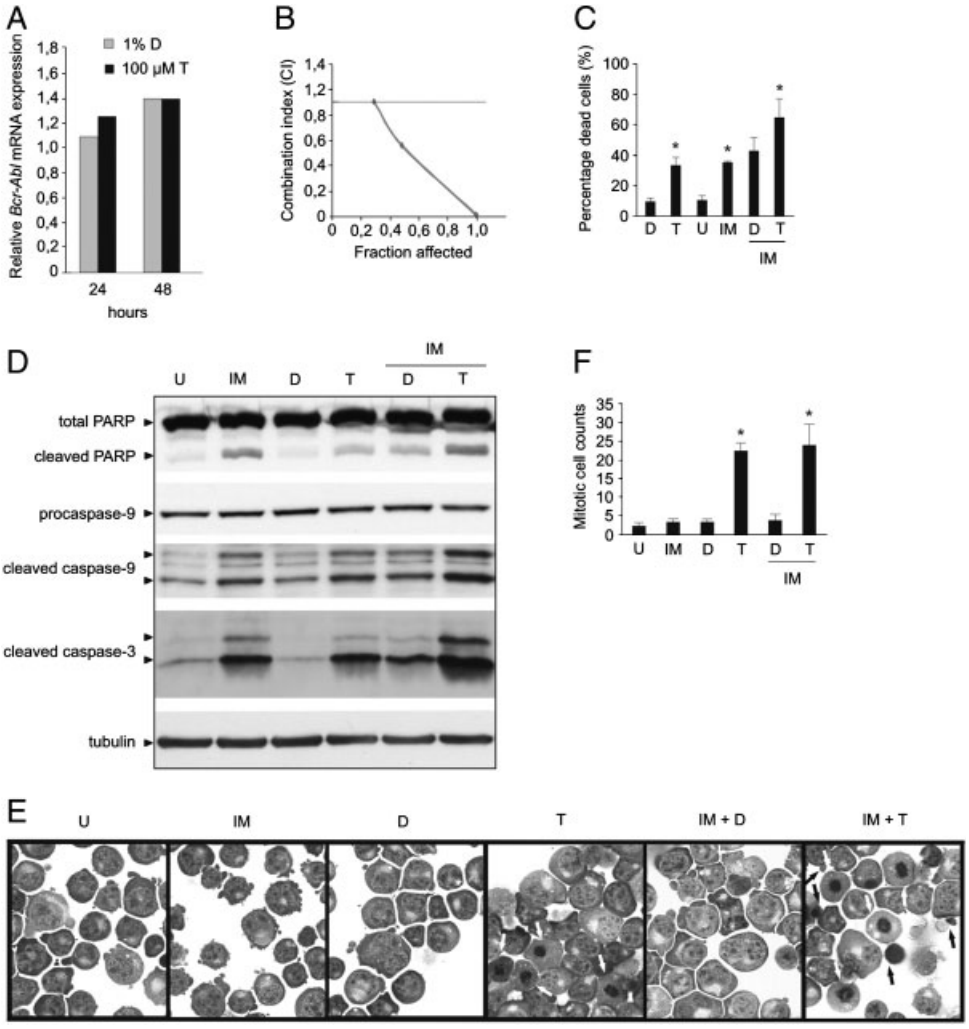

Figure 5. TAN interacts synergistically with imatinib to induce apoptosis in Bcr-Abl+ K562 cells. (A) The effect of TAN on the relative *BCR-ABL* expression was determined *via* quantitative RT-PCR. The cells were treated with 100 μM or 1% DMSO (solvent control) for 24 and 48 h. (B) K562 cells were treated with different concentrations of imatinib and TAN at a constant ratio of 1/25 for 48 h. The CI was determined according to a commercially available software program CalcySyn (CI < 1 = synergism). This result is representative for three equivalent experiments. (C) K562 cells were exposed to coadministration of 40 μM TAN and 1.8 μM imatinib after which the percentage dead cells was determined on flow cytometry. (D–F) Exposure of K562 cells to 80 μM TAN, 0.8 μM imatinib, and/or cotreatment for 24 h. (D) Western blot analysis and staining with the antibodies for PARP, caspase-9, cleaved caspase-3 and tubulin. One representative blot is illustrated. (E) After treatment, cytospin slides were prepared, stained with May–Grünwald–Giemsa, and viewed under the microscope using a × 50 oil objective. Representative fields are shown; white arrowheads indicate mitotic arrested cells and black arrowheads apoptotic cells. (F) Quantification of the mitotic arrested cells is presented. Values represent the means for two independent determinations on a total of 100 cells for each condition. The bars indicate the SD with $p < 0.05$ (*).

DNA laddering fragmentation and the cleavage of PARP. Since pretreatment with the pancaspase inhibitor Z-VAD-FMK blocked caspase-3 activation, PARP cleavage and G_2/M arrest, but failed to restore the viability of the K562 cells, caspase activation seemed not to be the essential event during TAN-induced cell death. This suggested that apart from apoptosis other mechanisms might contribute to cell death induced by TAN as a reaction to excessive ER stress. We could demonstrate that TAN-induced apoptosis was preceded by activation of the proapoptotic arm of the UPR. Since it is accepted that procaspase-4 associates with IRE1 and is a prominent initiator caspase coupled with terminal UPR induction, we investigated its activation [24, 25]. However, we could not demonstrate caspase-4 activation (data not shown). This can be explained by the fact that activation of caspase-12 or caspase-4 is not always required for caspase-dependent ER-stress apoptosis [26]. Nevertheless, all the other players of the UPR (XBP1 splicing, Grp78 and CHOP upregulation) were involved which are in favor of ER stress-induced apoptosis.

In contrast to our results, TAN is also able to activate the 'adaptive UPR' under certain circumstances. Previous research performed by Takano *et al.* [27] showed that methoxyflavones have strong protective effects against ER stress. TAN's protective effects were associated with enhanced expression of UPR target genes (*GRP78* and *CHOP*) and phosphorylation of eIF2α. The reason why in our study TAN activates the "terminal UPR" may be explained by the dose used in the experiments, 100 μM TAN in contrast to a maximum of 40 μM by Takano *et al.* Recently, Piwocka *et al.* [28] demonstrated that the Bcr-Abl fusion protein is a strong modulator of the ER calcium release. Expression of Bcr-Abl correlated with a decreased amount of ER releasable calcium and higher expression of GRP78 and CHOP compared with non-Bcr-Abl expressing cells. Therefore, it is not surprising that specific inhibition of Bcr-Abl with imatinib increased the ER releasable calcium. Moreover, the ER-associated caspase-12 was activated during imatinib-induced apoptosis [28, 29].

Furthermore, the potential of ER stress-induced cell death in Bcr-Abl+ K562 cells and CML was recently highlighted by the synergism between arsenic trioxide-induced ER stress and imatinib-induced intrinsic apoptosis where coadministration resulted in increased upregulation of GRP78, CHOP, ATF6 levels, and processing of caspase- 7, -8 and -9 [30]. Inspired by these results, we investigated the combination of TAN and imatinib in K562 cells. We found a synergistic cytotoxic effect evidenced by an accumulation of apoptotic cells and cells in mitotic arrest, and stronger effects on caspase activation.

In conclusion, our results suggest that the flavonoid TAN is an inducer of a G_2/M arrest and of cell death, with signs of both classical mitochondrial caspase-9-mediated and of ER stress-mediated apoptosis. Furthermore, TAN shows a synergistic cytotoxic effect combined with imatinib. We hypothesize that the ER is a genuine target to tackle in Bcr-Abl+ leukemias and suggest that the synergism of ER stress inducers and tyrosine kinase inhibitors has potential for further investigation.

The authors wish to thank Roselien Schelfaut and Jean Roels van Kerckvoorde for their excellent technical assistance. BV was supported by the Vlaamse Liga tegen Kanker (E. Verscheuren Fonds) and by the Concerted Research Initiative of the Ghent University (GOA project 01G013A7). MVG is a postdoctoral fellow of the Fund for Scientific Research-Flanders (Belgium). Imatinib was kindly provided by Elisabeth Buchdunger (Novartis Pharma, Basel, Switzerland).

The authors have declared no conflict of interest.

5 References

[1] Birt, D. F., Hendrich, S., Wang, W., Dietary agents in cancer prevention: flavonoids and isoflavonoids. *Pharmacol. Ther.* 2001, *90*, 157–177.

[2] Bracke, M., Vyncke, B., Opdenakker, G., Foidart, J. M. *et al.*, Effect of catechins and citrus flavonoids on invasion *in vitro*. *Clin. Exp. Metastasis* 1991, *9*, 13–25.

[3] Bracke, M. E., Bruyneel, E., Vermeulen, S. J., Vennekens, K., Citrus flavonoid effect on tumor invasion and metastasis. *Food Technol.* 1994, *48*, 121–124.

[4] Bracke, M. E., Boterberg, T., Depypere, H., Stove, C. *et al.*, in: Buslig, B., Manthey, J. (Eds.), *Flavonoids in Cell Function*, Kluwer Academic/Plenum Publishers, New York 2002, pp. 135–139.

[5] Chen, K.-H., Weng, M.-S., Lin, J.-K., Tangeretin suppresses IL-1ß-induced cyclooxygenase (COX)-2 expression through inhibition of p38 MAPK, JNK, and AKT activation in human lung carcinoma cells. *Biochem. Pharmacol.* 2007, *73*, 215–227.

[6] Pan, M.-H., Chen, W.-J., Lin-Shiau, S.-Y., Ho, C.-T., Lin, J.-K., Tangeretin induces cell-cycle G1 arrest through inhibiting cyclin-dependent kinases 2 and 4 activities as well as elevating Cdk inhibitors p21 and p27 in human colorectal carcinoma cells. *Carcinogenesis* 2002, *23*, 1677–1684.

[7] Hirano, T., Abe, K., Gotoh, M., Oka, K., Citrus flavone tangeretin inhibits leukemic HL-60 cell growth partially through induction of apoptosis with less cytotoxicity on normal lymphocytes. *Br. J. Cancer* 1995, *72*, 1380–1388.

[8] Yeh, T.-C., Chiang, P. C., Li, T. K., Hsu, J. L. *et al.*, Genistein induces apoptosis in human hepatocellular carcinomas *via* interaction of endoplasmic reticulum stress and mitochondrial insult. *Biochem. Pharmacol.* 2007, *73*, 782–792.

[9] Park, J. W., Woo, K. J., Lee, J. T., Lim, J. H. *et al.*, Resveratrol induces pro-apoptotic endoplasmic reticulum stress in human colon cancer cells. *Oncol. Rep.* 2007, *18*, 1269–1273.

[10] Boelens, J., Lust, S., Offner, F., Bracke, M. E., Vanhoecke, B. W., The endoplasmic reticulum: a target for new anticancer drugs. *In Vivo* 2007, *21*, 215–226.

[11] Druker, B. J., Translation of the Philadelphia chromosome into therapy for CML. *Blood* 2008, *112*, 4808–4817.

[12] Lust, S., Vanhoecke, B., Van Gele, M., Boelens, J. *et al.*, Xanthohumol kills B-chronic lymphocytic leukemia cells by an apoptotic mechanism. *Mol. Nutr. Food Res.* 2005, *49*, 844–850.

[13] Vandesompele, J., De Paepe, A., Speleman, F., Elimination of primer-dimer artifacts and genomic coamplification using a two-step SYBR green I real-time RT-PCR. *Anal. Biochem.* 2002, *303*, 95–98.

[14] Vandesompele, J., De Preter, K., Pattyn, F., Poppe, B. *et al.*, Accurate normalization of real-time quantitative RT-PCR data by geometric averaging of multiple internal control genes. *Genome Biol.* 2002, *18*, RESEARCH0034.

[15] Pattyn, F., Speleman, F., De Paepe, A., Vandesompele, J., RTPrimerDB: the real-time PCR primer and probe database. *Nucleic Acids Res.* 2003, *31*, 122–123.

[16] Ding, L., Yan, J., Zhu, J., Zhong, H. *et al.*, Ligand-independent activation of estrogen receptor α by XBP-1. *Nucleic Acids Res.* 2003, *31*, 5266–5274.

[17] Chou, T.-C., Talalay, P., Quantitative analysis of dose-effect relationships: the combined effects of multiple drugs or enzyme inhibitors. *Adv. Enzyme Regul.* 1984, *22*, 27–55.

[18] Chou, T.-C., in: Chou, T.-C., Rideout, D. C. (Eds.), *Synergism and Antagonism in Chemotherapy*, Academic Press, San Diego 1991, pp. 61–102.

[19] Jacquel, A., Herrant, M., Legros, L., Belhacene, N. *et al.*, Imatinib induces mitochondria-dependent apoptosis of the Bcr-Abl-positive K562 cell line and its differentiation toward the erythroid lineage. *FASEB J.* 2003, *17*, 2160–2162.

[20] Sawafuji, K., Miyakawa, Y., Kizaki, M., Ikeda, Y., Cyclosporin A induces erythroid differentiation of K562 cells through p38 MAPK and ERK pathways. *Am. J. Hematol.* 2003, *72*, 67–69.

[21] Herrera, R., Hubbell, S., Decker, S., Petruzzelli, L., A role for the MEK/MAPK pathway in PMA-induced cell cycle arrest: modulation of megakaryocytic differentiation of K562 cells. *Exp. Cell Res.* 1998, *238*, 407–414.

[22] Danial, N. N., BCL-2 family proteins: critical checkpoints of apoptotic cell death. *Clin. Cancer Res.* 2007, *13*, 7254–7263.

[23] Denoyelle, C., Abou-Rjaily, G., Bezrookove, V., Verhaegen, M. *et al.*, Anti-oncogenic role of the endoplasmic reticulum differentially activated by mutations in the MAPK pathway. *Nat. Cell. Biol.* 2006, *8*, 1053–1063.

[24] Nakagawa, T., Zhu, H., Morishima, N., Li, E. *et al.*, Caspase-12 mediates endoplasmic-reticulum-specific apoptosis and cytotoxicity by amyloid-ß. *Nature* 2000, *403*, 98–103.

[25] Hitomi, J., Katayama, T., Eguchi, Y., Kudo, T. *et al.*, Involvement of caspase-4 in endoplasmic reticulum stress-induced apoptosis and Aß-induced cell death. *J. Cell Biol.* 2004, *165*, 347–356.

[26] Obeng, E. A., Boise, L. H., Caspase-12 and caspase-4 are not required for caspase-dependent endoplasmic reticulum stress-induced apoptosis. *J. Biol. Chem.* 2005, *280*, 29578–29587.

[27] Takano, K., Tabata, Y., Kitao, Y., Murakami, R. *et al.*, Methoxyflavones protect cells against endoplasmic reticulum stress and neurotoxin. *Am. J. Physiol. Cell Physiol.* 2007, *92*, C353–C361.

[28] Piwocka, K., Vejda, S., Cotter, T. G., O'Sullivan, G. C., McKenna, S. L., Bcr-Abl reduces endoplasmic reticulum releasable calcium levels by a Bcl-2-independent mechanism and inhibits calcium-dependent apoptotic signaling. *Blood* 2006, *107*, 4003–4010.

[29] Pattacini, L., Mancini, M., Mazzacurati, L., Brusa, G. *et al.*, Endoplasmic reticulum stress initiates apoptotic death induced by STI571 inhibition of p210 bcr-abl tyrosine kinase. *Leuk. Res.* 2004, *28*, 191–202.

[30] Du, Y., Wang, K., Fang, H., Li, J. *et al.*, Coordination of intrinsic, extrinsic, and endoplasmic reticulum-mediated apoptosis by imatinib mesylate combined with arsenic trioxide in chronic myeloid leukemia. *Blood* 2006, *107*, 1582–1590.

